NANOSTRUCTURING THROUGH LASER MANIPULATION*

F. TANTUSSI, N. PORFIDO, F. PRESCIMONE, F. FUSO,
E. ARIMONDO, M. ALLEGRINI

CNISM, INFM/CNR polyLab, Dipartimento di Fisica Enrico Fermi, Università di Pisa
Largo B. Pontecorvo 3, I-56127, Pisa, Italy

We have developed a nanofabrication approach that exploits laser manipulation to guide neutral atoms, belonging to a well collimated beam, into regularly spaced positions prior to deposition onto a substrate. The method can be straightforwardly adapted to structured deposition in the low substrate coverage regime. Results demonstrate the achievement of isolated nanostructures with lateral size in the 10 nm range.

1. Introduction

The relentless search for miniaturization prompts the need for new fabrication techniques in many technological fields. Different strategies and alternative methods have been proposed, developed and, in some cases, introduced into the industrial environment to push resolution down to the few nanometers range, thus overcoming the limitations of conventional techniques. Besides the need for enhancing space resolution, a strong interest is growing for developing bottoms-up methods [1]. Contrary to conventional top-down techniques, where structuring is typically achieved by removing or modifying laterally defined patterns, bottoms-up implies matter manipulation right before, or during, the structure formation. Such new technologies promise radical changes in the fabrication strategies, allowing an unprecedented control on microstructure, stoichiometry and morphology. Advanced applications ranging through, for instance, precise doping of materials for spintronic purposes to hybrid molecular electronics will take advantage of the precise lateral definition and of the virtual absence of any unwanted material damage offered by such techniques. Methods based on scanning probe microscopy (SPM) have been demonstrated able to manipulate matter down to the single atom level [2]; however, SPM techniques are typically cumbersome to be realized and suffer from their inherently serial, hence slow, character.

* This work has been partially supported by EC through FET-IST "Nanocold" and by Fondazione Cassa di Risparmio di Pisa under the Scientific Project PR05/137.

In the fundamental areas of laser physics, atomic spectroscopy and metrology, many efforts have been devoted to control the dynamical properties of atoms and molecules in the vapor phase [3], that led to a number of important advancements including, e.g., production of Bose-Einstein condensates and introduction of atom lasers. Atom optics techniques represents a viable route to nanofabrication thanks to the highly accurate matter control that can be achieved. The inherently non-obtrusive character of light and the possibility to develop parallel schemes are additional appealing features ensured by laser manipulation.

2. Laser manipulation tools

Application of laser manipulation tools to fabrication brought the development of atomic nanofabrication (ANF [4,5]), also known as atom lithography. Roughly speaking, in ANF the role of matter and light is reversed with respect to conventional optical lithography: a beam of atoms (the matter) is in fact used to produce nanostructures through conditioning by laser radiation (the light). As in electron lithography, the sub-nm de Broglie wavelength of the atom beam prevents diffraction effects to play a remarkable role. Moreover, the process involves low kinetic energy particles, hence detrimental effects like backscattering or sputtering are virtually absent; contrary to charged beam lithography, any issue related with Coulomb repulsion can be neglected as well.

Pioneering implementations of ANF used sodium, and, later on, chromium to create arrays of regular nanolines with lateral size in the tens of nm range [6,7]. Suitable particle-sensitive resists were then introduced, mostly based on self-assembled monolayers (SAM), whose impression allows transferring the pattern created by laser manipulation onto the underlying substrate [8].

The main mechanism of ANF is the occurrence of a conservative force, called dipolar force, following the interaction of an atom with a standing electromagnetic field at a wavelength quasi-resonant with an atomic transition. Such a force, classically similar to that felt by electric dipoles immersed in non homogeneous fields, stems from the space modulated light shift for the energy levels of the atom dressed by the external field [4,5]. Assuming a standing wave with an intensity variation along the x-axis, $I(x)$, as produced by retro-reflecting a single laser beam (1-D standing wave), the force $F(x)$ is [4]

$$F(x) \approx -\frac{\hbar\Gamma^2}{8\delta I_s}\frac{\partial I(x)}{\partial x} \qquad (1)$$

where Γ and I_S are the natural rate and the saturation intensity for the considered atomic transition, respectively, and δ is the detuning from resonance. Let us consider an atom travelling along a direction orthogonal to the x-axis: its transverse dynamics will be modified by the dipolar force and the atom will be pushed towards the antinodes, or nodes, of the standing wave, depending on the sign of the detuning. Therefore, an initially homogeneous beam will be spatially segregated into an array of parallel planes spaced exactly half the wavelength. More complex field geometries, e.g., produced by superposing three or more laser beams, lead to differently shaped arrays, consisting for instance of regularly spaced hexagonal or circular dots [4].

In absolute terms, the dipolar force of Eq. (1) is typically weak. In fact, detuning δ cannot be set arbitrarily low in order to prevent photon absorption and consequent re-emission, which would produce atom heating and subsequent lack of control in the atom dynamics. For the guiding mechanism to be effective, the transverse velocity of the atoms must be very small, hence highly collimated beams are typically required in ANF, with residual divergence in the mrad range. In order to preserve atom beam density, i.e., to achieve exposure times compatible with practical applications, collimation cannot be attained by simple mechanical means. Laser manipulation tools are used also to this purpose based, e.g., on 2-D optical molasses [3] able to decrease the beam transverse temperature below the mK range.

3. Experimental

Our implementation of ANF operates with cesium atoms and exploits a 1-D standing wave as the light mask. The setup [9-11] has been designed and built to satisfy all basic requirements of ANF; moreover, contrary to all systems reported in the literature, it includes a modified magneto-optical trap (MOT) working as an atom funnel to produce a longitudinally cooled atom beam [10]. Main motivations to such a design choice are: (i) to access the mostly unexplored deposition regime involving arrival of low kinetic energy atoms onto a surface; (ii) to achieve long interaction times in both collimation (optical molasses) and atom guiding (light mask) stages thanks to the small velocity of the beam (around 10 m/s [10]); (iii) to realize straightforward operation in the low particle density regime. In fact, due to the use of specific laser interaction schemes, the dynamical properties of the atoms are almost deterministically assigned independently of the particle density. Therefore, deposits consisting of few atoms can be attained by reducing the atom flux through externally accessible parameters (e.g., laser power, magnetic field, background vapor density).

The system has already proven its capabilities in resist-assisted fabrication of parallel nanotrenches in gold [11], spaced exactly one half the wavelength ($\lambda/2$ = 426 nm, in our case). In those experiments, the space segregated atom beam was used to impress a particle sensitive film consisting of a self-assembled monolayer of alkylthiol molecules grown on gold. Arrival of cesium atoms, at a dose above 2 atoms per molecule, inhibited protection; a subsequent wet etching process led to nanotrench formation. Size and morphology of the nanotrenches revealed a strong influence of the underlying layers. In particular, the homogeneity of the SAM, ruled in turn by the graininess of the gold layer, posed a limitation in the maximum achievable space resolution (40-50 nm [11]).

In order to unravel the intriguing phenomena underlying nanostructure growth in ANF conditions, direct deposition from the structured Cs beam was accomplished on different substrates. Results presented here refer in particular to highly oriented pyrolitic graphite (HOPG) and monolayers of nonanethiol molecules self-assembled onto a thin (100 nm) flame-annealed gold film on mica. Thanks to a tunneling microscope (STM) head (Omicron LS-STM equipped with Dulcinea Nanotec controller [12]), installed in the same ultra-high vacuum deposition chamber, the properties of the deposited samples could be detected without any need for sample exposure to air.

4. Results and discussion

Many different results have been obtained in a large series of experiments: a few of them will be presented and briefly discussed here. Our experiments were aimed at exploring the regime of moderate to low substrate coverage, meaning that the flux density of the laser-cooled atom beam, time integrated over the whole duration of the exposure, was typically kept below the value corresponding to the growth of a single Cs layer. It must be noted that, due to the number of structural variants possible for Cs on graphite [13], there is no unambiguous definition of the coverage ratio. Results presented here refer to a time integrated flux density corresponding to arrival, on the average, of 0.05-0.20 Cs atoms per single graphite carbon atom. In practical terms, this roughly corresponds to 100-300 min exposure time at an atom flux around 10^8 atoms/s over a 25-40 mm^2 area. Due to the relatively long duration of the deposition process, special care has been devoted to mechanical stability and immunity against thermal drifts of the deposition setup, concerning in particular the relative alignment between the standing wave and the substrate.

Thanks to the long interaction time experienced by the slow atoms crossing the standing wave, the so-called channeling regime is realized. In such conditions, atoms are forced to oscillate in the transverse direction; those oscillations confine the particles in an array of channels, spaced exactly one half the wavelength, whose width can be numerically evaluated. Figure 1 reports results of numerical simulations of the atom trajectories based on a semiclassical model accounting for spatially modulated light shifts of the atom levels and for the possibility of spontaneous emission following off-resonance photon absorption. Parameters are in agreement with the experiment; channeling is efficiently achieved, the channel width being on the order of 40-60 nm.

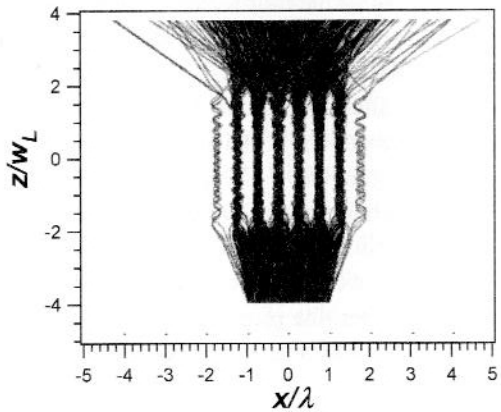

Figure 1. Results of the numerical simulation for 150 atom trajectories. The atom beam, assumed to possess a 10 mrad initial divergence, moves along the z-direction (from the bottom to the top of the graph) and interacts with a standing wave directed along the x-direction, assumed to be focused on a waist w_L (typically, w_L ~ 50-100 μm). Channeling and spatial segregation on a $\lambda/2$ scale are evident. The peak intensity of the standing wave was set to 20 mW/cm^2 and its detuning was δ = 1 GHz.

Fabrication of a regular array of cesium nanolines should then be expected; however, the reduced substrate coverage achieved in the experiment prevents formation of continuous lines, leading instead to the growth of isolated nanostructures. This is demonstrated for instance in Fig. 2(a), showing the STM current map of a HOPG substrate exposed to the structured Cs beam. Spots observed in the scan, absent in the pristine substrate and attributed to Cs structures, are mutually aligned along a direction orthogonal to the standing wave vector, with a spacing compatible with the expected $\lambda/2$ value [see the line profile in Fig. 2(b)]. The deposited material is unevenly distributed over the substrate: such a finding is a clear signature of surface processes occurring at the interaction of the deposited atoms with the substrate [14]. In particular,

surface diffusion is expected to occur; energy barriers in the diffusive motion (e.g., Ehrlich-Schwoebel barriers) have been already considered as one of the main ingredients in defining the morphology of ANF-produced structures [15]. Moreover, we cannot completely rule out the possibility of atom penetration into graphite: intercalation by alkali atoms is a well known process [13].

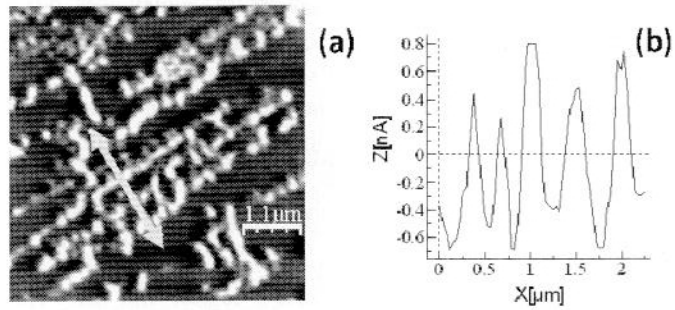

Figure 2. Tunneling current map of a sample deposited onto HOPG (a); profile analysis along the segment superposed to the map (represented as a double arrow), demonstrating line spacing compatible with $\lambda/2$ = 426 nm (b). The segment direction coincides with the standing wave vector. The estimated coverage ratio of the deposition was ~0.05.

High-resolution STM topography investigations reveal that substrate features affect nanoisland shape and location. The map shown as an example in Fig. 3(a) clearly demonstrate that Cs deposits are mainly found in the proximity of HOPG steps, i.e., naturally occurring fractures between atomically flat terraces. We found a relationship between height of the steps and adsorbed Cs: islands are not observed close to steps smaller than approximately 0.1 nm, roughly corresponding to 2-4 graphene sheets. Moreover, nanoislands appear further structured in small droplets [see the magnified scan in Fig. 3(b)].

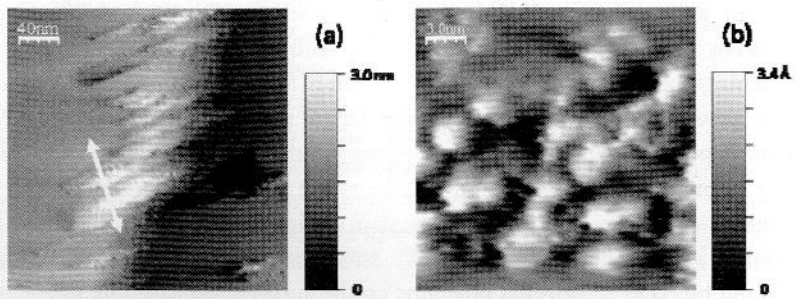

Figure 3. STM topography of a sample deposited onto HOPG (a) and magnification of a Cs nanostructure (b). The double arrow superposed to the left map marks the direction of the standing wave vector. The estimated coverage ratio of the deposition was ~0.15.

Nanoislands fabricated on HOPG systematically exhibit a peculiar "cigar-like" shape, with transverse size on the order of 10 nm, or even less, and typical height of a few nm. Their length is variable in the approximate range 10-200 nm, being strongly dependent on the presence of substrate features. Remarkably, the long axis of the "cigars" was always almost perfectly aligned orthogonally with the standing wave direction; such a behavior, which was not found in depositions carried out without the light mask, represents a definite demonstration of the atom guiding effect due to the presence of the standing wave. Moreover, large size scans demonstrate that the distribution of the deposited material follows the $\lambda/2$ spacing imposed by the standing wave [17].

Changing the substrate material can assess the role played by surface properties in ruling nanostructure morphology. Indeed, deposition on the molecular substrate (SAM), as shown for instance in Fig. 4(a), did not reveal "cigar-like" islands, but mostly linear structures tens of nm wide.

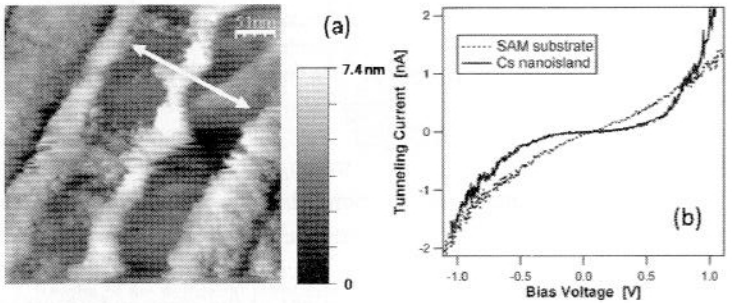

Figure 4. STM topography of a sample deposited onto SAM (a) and *IV* curves acquired on different positions of a deposited sample (b). The double arrow superposed to the map marks the direction of the standing wave vector. The estimated coverage ratio of the deposition was ~0.2.

Interaction between alkali atoms and SAM has been investigated in the past mostly to assess the particle impression process [4,8]. Recently appeared calculations [16] suggest that cesium atoms tend to get ionic character while approaching the substrate because of Coulomb forces. So-produced ions can then be accelerated towards the substrate, hence penetrating through the SAM network; upon arrival onto the underlying gold surface, energy is released leading to break the thiol/Au bond. We have not found any clear evidence for molecular damage in our morphological investigations. Further confirmation was found in local tunneling current vs bias measurements (*IV* spectroscopy) carried out by STM in selected positions on the surface. An example is given in Fig. 4(b), where the *IV* curve captured on a region not covered by Cs is

compared with that acquired over a Cs nanoisland, almost spherically shaped with diameter of a few nm. The expected *IV* behavior for a SAM layer grown over gold was found when analyzing uncoated regions, whereas tunneling through the Cs nanoisland appears inhibited in a relatively large bias range across zero. Such a finding can be explained in terms of Coulomb blockade [1], demonstrating that the Cs nanoisland behaves like a metallic nanocapacitor (estimated capacitance 0.3 aF) able to feel single electron charge processes.

5. Conclusions

Thanks to its ability in governing the dynamical properties of neutral atoms, laser manipulation is a viable candidate for the development of novel nanofabrication techniques. Our results confirm that laser manipulation tools can be exploited to produce isolated nanostructures, with a typical minimum size in the ten nm range. Further work, supported by the continuous advancements in laser technologies, will address applications to technologically relevant materials, such as semiconductors or dopant species, in order to set the basis for a new approach in precise doping and hybrid molecular electronics.

References

1. For a review, see, for instance: R. Waser Ed., *Nanoelectronics and Information Technology* (Wiley-VCH, Weinheim, 2005).
2. B. Bushan, Ed., *Springer Handbook of Nanotechnology* (Springer, New York, 2007).
3. H. Metcalf and P. van der Straten, *Laser Cooling and Trapping* (Springer, New York, 2001).
4. D. Meschede and H. Metcalf, J. Phys. D: Appl- Phys. D **36**, R17 (2003).
5. M.K. Oberthaler and T. Pfau, J. Phys.: Condens. Matter **15**, R233 (2003).
6. G. Timp, et al., Phys. Rev. Lett. **69**, 1636 (1992).
7. J.J. McClelland, et al., Science **262**, 87 (1993).
8. K.K. Berggren, et al., Science **269**, 1255 (1995).
9. F. Tantussi, et al., Mat. Sci. Eng. C **27**, 1418 (2007).
10. A. Camposeo, et al., Opt. Commun. **200**, 231 (2001).
11. C. O'Dwyer, et al., Nanotechnology **16**, 1536 (2005).
12. I. Horcas, et al., Rev. Sci. Instrum. **78**, 013705 (2007).
13. M. Caragiu and S. Finberg, J. Phys.: Condens. Matter **17**, R995 (2005).
14. J.A. Venables, *Surface and Thin Film Processes* (Cambridge University Press, Cambridge, 2000).
15. F. Nita and A. Pimpinelli, J. Appl. Phys. **97** 113529 (2005).
16. C. Di Valentin, et al., J. Phys. Chem. **109**, 1815 (2005).
17. F. Tantussi, et al., Appl. Surf. Sci, in press (2008).